

Microtremors HVSR Correlation with Sub Surface Geology and Ground Shear Strain at Palu City, Central Sulawesi Province, Indonesia

PyiSoe Thein, Subagyo Pramumijoyo, Kirbani Sri Brotopuspito, Junji Kiyono, Wahyu Wilopo and Agung Setianto

Abstract – In the present study, we have performed microtremor measurements at Palu City, Indonesia for HVSR correlation, which will be used in seismic hazard mapping. We found the correlation between subsurface geology and microtremors HVSR, even in complex geological settings. Considering the damage produced by the 2005 Palu earthquake (Mw 6.3), we also estimated seismic vulnerability index and ground shear strain distribution at Palu City. We believe that the surface geological conditions also reflected in the variations of the resonance frequencies of the soils. Microtremor survey results showed that in hilly areas had low seismic vulnerability index, whereas in coastal alluvium was composed of material having a high seismic vulnerability indication. Understanding the parameters of sedimentary layers, seismic vulnerability index and ground shear strain are very important for seismic hazard mitigation and environmental planning in Palu City.

Keywords – Microtremor, Sedimentary Layers, Seismic Vulnerability Index, Ground Shear Strain, Palu City.

I. INTRODUCTION

Sulawesi Island, eastern Indonesia, is located at the junction between the converging Pacific-Philippine, Indo-Australian Plates and the Sundaland, i.e. the south-eastern part of the Eurasian Plate. The Central Sulawesi Fault System, one of the major structures in SE Asia, cuts across Sulawesi Island from NW to SE, connecting the North Sulawesi subduction zone to the Banda Sea deformation zones.

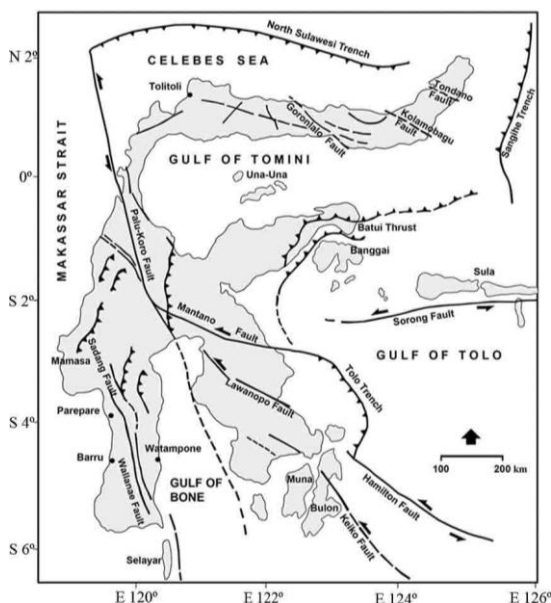


Fig. 1. Tectonic map of Sulawesi [1].

One of the major structures in Central Sulawesi is the Palu- Koro Fault system, which extends NNW- SSE direction and cross cuts Sulawesi along more than 300 km, from the North Sulawesi trench pass through Palu Bay, southward turn to the SE connect to the Matano and Lawanopo Faults and further eastward, both faults join to Tolo trench (Figure 1) [1]. In this study, Palu, where a large earthquake is expected in the near future, is considered to be a target area. We carried out higher density single point observations and larger radius array observations. Based on the observed data, we calculated the distribution of the predominant and phase velocities of the Rayleigh wave.

II. GEOLOGY

Sulawesi, Eastern Indonesia, is a K-shaped island lying at the junction of Eurasia, Indo-Australian and Pacific plates, in a complex region where subduction and collision have been and are still active. Based on the occurrence of distinct rock assemblages, the island can be subdivided into three main geological provinces, namely: (i) West Sulawesi, where Tertiary sediments and magmatic rocks are prominent, (ii) Central and South-East Sulawesi, mainly made up of Early Cretaceous metamorphic rocks and (iii) East Sulawesi, where a huge ophiolitic nappe rests on Mesozoic and Paleozoic sedimentary rocks. The West Sulawesi magmatic province includes the southern arm of Sulawesi, the Western part of Central Sulawesi and finally the Northern arm which extends from Palu to the Manado area [2], [3]. Evolution of Neogene kinematics along the Palu-Koro fault was confirmed based on microtectonics approach, i.e., sinistral strike-slip due to E-W compression, radial extensions caused by telescoping vertical movement of Neogene granitoid, and then left lateral with normal component displacement due to N-S extension/ E-W compression which is still active actually [4]. Palu depression area is filled by most of clay, silt, and sand deposits as alluvial deposits except on the border east or west consist of gravelly sands as colluvial wedges. The composition of gravel is granitic fragment to the northwest, mostly of schist on the west and to the east the gravel consists of schist, igneous and sedimentary rocks. West escarpment to the north consists of granite and granodiorite units, and to the south consists of schist-phyllitic units. East escarpment consists of molasses [5].

III. SUBSURFACE PROFILE FROM BOREHOLES

The subsurface soil profiles and related geotechnical parameters have been evaluated in three sites for determination strong ground motion and ground response analyses.

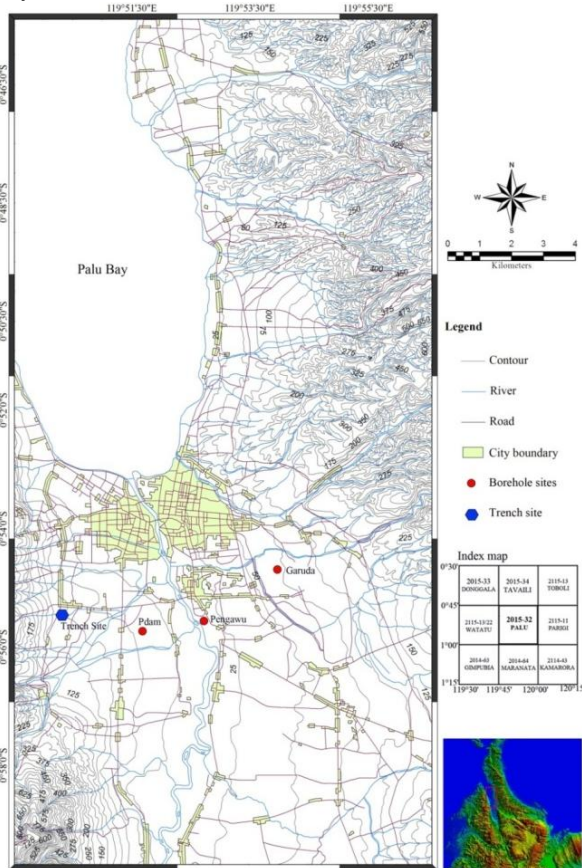


Fig.2. Locations of the trench and boreholes in Palu area.

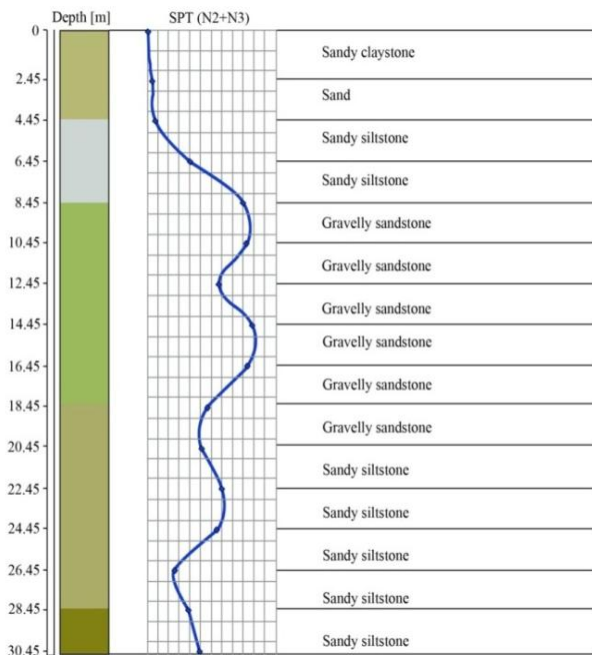


Fig.3. Soil Profile of Garuda.

The detailed drilling program had been carried out for subsurface investigation in Palu basin. There are three boreholes throughout the basin especially in Palu area to evaluate the geotechnical properties of subsurface soil layers (Figure 2). The boreholes were generally drilled up to the bedrock. The depths are varying from 1 m to 30 m. The subsurface soil profiles and soil types are determined according to United State Soil Classification (USCS) system, based on grained size analysis, Atterberg's Limits Test and drill logs. The evaluated subsurface profiles for each area in the basin are shown in the following figure 3. The geotechnical parameters for each layer in respective subsurface soil profile had been evaluated and described in Table 1.

Table 1 Geotechnical properties of each subsurface layer at Garuda.

Layer	Thickness(m)	Soil & rock type
1	0.00 - 2.45	Sandy claystone
2	2.45 - 4.45	Sand
3	4.45 - 6.45	Sandy siltstone
4	6.45 - 8.45	Sandy siltstone
5	8.45 - 10.45	Gravelly sandstone
6	10.45- 12.45	Gravelly sandstone
7	12.45- 14.45	Gravelly sandstone
8	14.45- 16.45	Gravelly sandstone
9	16.45- 18.45	Gravelly sandstone
10	18.45- 20.45	Gravelly sandstone
11	20.45-22.45	Sandy siltstone
12	22.45- 24.45	Sandy siltstone
13	24.45- 26.45	Sandy siltstone
14	26.45- 28.45	Sandy siltstone
15	28.45- 30.45	Sandy siltstone

IV. MICROTREMOR ARRAY OBSERVATION

We carried out array observations at eight sites in Palu City (Figure 4). Microtremor array survey was conducted by four accelerometers at several districts in Palu City. Four accelerometers were used in each array observation site. One was installed at a center of the circle with a radius, r. Other three were arranged on the circle with a shape of regular triangle. Observation duration time was 20-30 minutes and sampling frequency was 100Hz. Sequential observations were conducted three times by changing the array radius; r=3, 10 and 30 meters. Then, a substructure profile was identified from the dispersion curve by using the Particle Swarm Optimization [6]-[8].

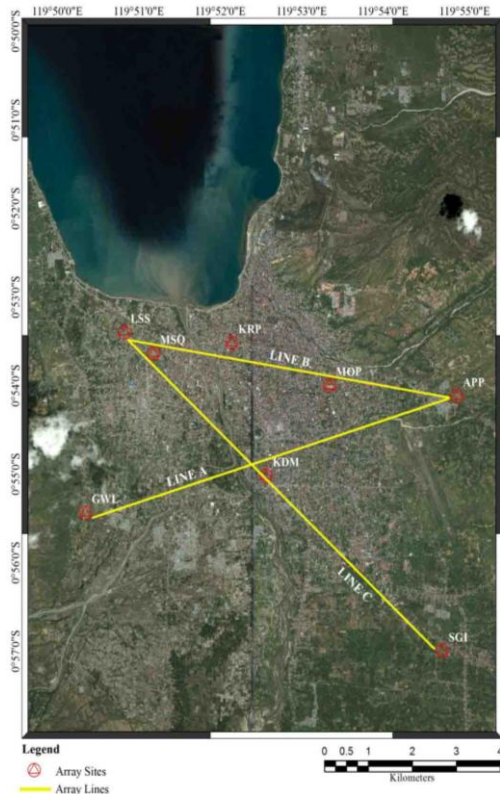


Fig.4. Three survey lines for array observation (Line A, Line B, and Line C)

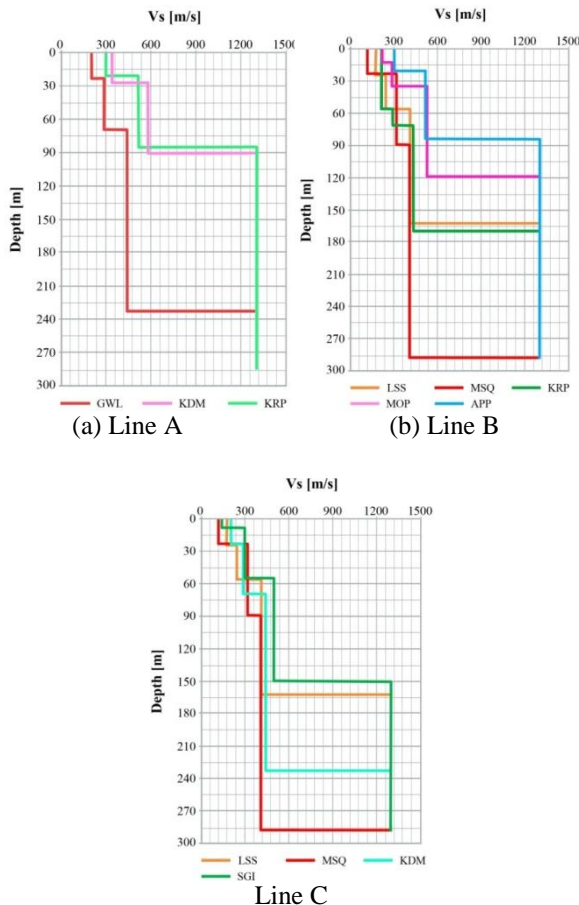


Fig.5. Vs structures of the ground along the survey lines (a) Line A, (b) Line B and (c) Line C.

For line A, the phase velocity corresponding to shallow ground with a high frequency range is about 369 m/s at APP, about 423 m/s at GWL, about 318 m/s at KDM, about 318 m/s at KRP, about 279 m/s at LSS, about 348 m/s at MOP, about 285 m/s at MSQ and about 317 m/s at SGI. The soft ground extended beneath LSS, which is the nearest site to the coast. The ground beneath the sites higher than GWL has relatively hard surface soil compared with the plain along the coast. Since the minimum phase velocity in the high frequency range is around 300 m/s, the soil profile is very similar along line B and line C. The dispersion curves obtained here had no discrepancies in the distribution of topography, altitude and predominant period. Figure 5 shows Vs structures of the ground along the survey lines (a) Line A, (b) Line B and (c) Line C. The outline of the SPAC method for the phase velocity calculation of Rayleigh waves follows.

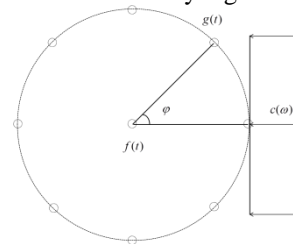


Fig.6. Microtremor array observation Schema.

$$F(\omega) = \frac{1}{2\pi} \int_{-\infty}^{\infty} f(t) \cdot \exp(-i\omega t) dt$$

$$= A_f(\omega) \cdot \exp(-i\phi_f(\omega)) \quad (1)$$

$$G(\omega) = \frac{1}{2\pi} \int_{-\infty}^{\infty} g(t) \cdot \exp(-i\omega t) dt$$

$$= A_g(\omega) \cdot \exp(-i\phi_g(\omega)) \quad (2)$$

$A_f(\omega)$, $A_g(\omega)$ and $\phi_f(\omega)$, are difference between the amplitude of $\phi_g(\omega)$, $F(\omega)$, $G(\omega)$ respectively. Further cross correlation in the frequency region of the two waveforms will be as follows.

$$CC_{fg} = F(\omega) \cdot \overline{G(\omega)} = A_f(\omega) \cdot A_g(\omega) \cdot \exp(i\Delta\phi(\omega)) \quad (3)$$

It shows the phase difference of $\Delta\phi(\omega)$

$$\Delta\phi(\omega) = \frac{\omega r}{c(\omega)} \quad (4)$$

$c(\omega)$ is the phase velocity from the phase difference.

$$CC_{fg} = A_f(\omega) \cdot A_g(\omega) \cdot \exp\left(i \frac{\omega r}{c(\omega)}\right) \quad (5)$$

The complex coherence of the two waveforms is defined by the following equation:

$$COH_{fg}(\omega) = \frac{CC_{fg}(\omega)}{A_f(\omega) \cdot A_g(\omega)} = \exp\left(i \frac{\omega r}{c(\omega)}\right) \quad (6)$$

$$\text{Re}\left(COH_{fg}(\omega)\right) = \cos\left(i \frac{\omega r}{c(\omega)}\right) \quad (7)$$

$$(\omega, \phi) = \frac{c(\omega)}{\cos\phi} \quad (8)$$

$$SPAC(\omega, r) = \frac{1}{2\pi} \int_0^{2\pi} \exp(i\omega r \frac{\omega r}{c(\omega)} \cos\phi) d\phi \quad (9)$$

$$Re(SPAC(\omega, r)) = \frac{1}{2\pi} \int_0^{2\pi} \cos(i\omega r \frac{\omega r}{c(\omega)} \cos\phi) d\phi \quad (10)$$

$$J\left(\frac{\omega r}{c(\omega)}\right) = \frac{1}{2\pi} \int_0^{2\pi} \exp(i\omega r \frac{\omega r}{c(\omega)} \cos\phi) d\phi \quad (11)$$

where $J_0(x)$ is the zero-order Bessel function of the first kind of x , and $c(\omega)$ is the phase velocity at frequency ω . The SPAC coefficient $\rho(r, \omega)$ can be obtained in the frequency domain using the Fourier transform of the observed microtremors.

$$Re(SPAC(\omega, r)) = J\left(\frac{\omega r}{c(\omega)}\right) \quad (12)$$

From the SPAC coefficient $\rho(r, \omega)$, the phase velocity is calculated for every frequency from the Bessel function argument of equation. 14 and the velocity model can be inverted.

Layer thickness and the average S-wave velocity in Figure 6 each array site. For the average S wave velocity model obtained by averaging the estimated ground structure of the array site was to be calculated by a weighted average using a S-wave velocity structure is estimated as a weighted layer thickness.

$$V_s = \sum V_{si} \frac{H_i}{H} \quad (13)$$

Figure 7 shows shear wave velocity map at Palu area.

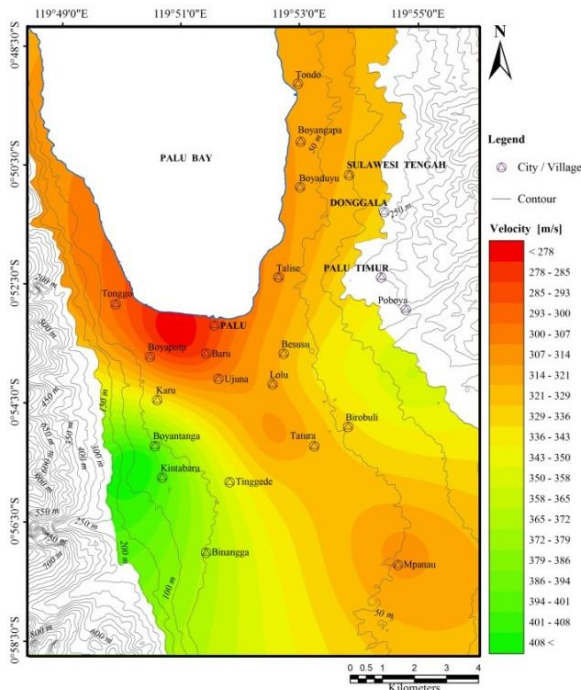


Fig.7. Shear wave velocity map at Palu area.

V. MICROTREMOR HVSR CORRELATION WITH SUBSURFACE GEOLOGY

The boundary depth was around 100-125 m and appeared very deep. In the west of the site, MSQ, the depth of the boundary drastically changed from 75-100 m

to 125 m. Rapid change can also be seen in the western part of the area near the GWL site because of the mountain location. Focusing on the site MSQ, although the elevation of surrounding area is almost at the same level, a sudden change in sedimentary layers can be seen. Figure 8 and 9 show soil profile at Mayor of Palu and three dimensional shape of the estimated subsurface structure. At present, since there are no detailed ground survey data in Palu such as deep boring, gravity anomalies, and seismic exploration, the existence of a hidden fault is just an estimation from microtremor observations. However, if a hidden fault exists beneath Palu City, we should prepare for a near-source earthquake here in Palu. Table 2 shows Estimation of the average shear wave velocity for array sites. For future work, additional dense array observations combined with other ground survey techniques need to be done to clarify the detailed subsurface structure, especially around the GWL site.

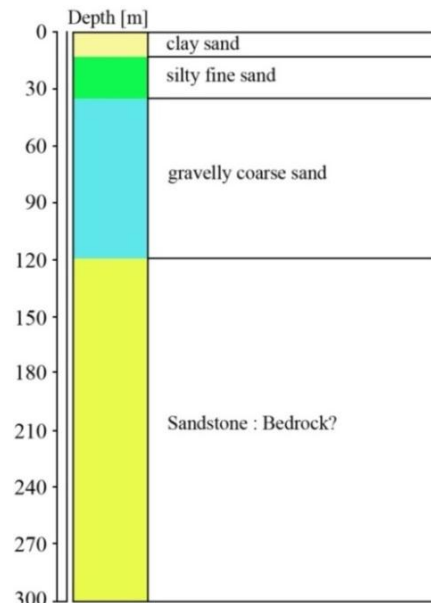


Fig.8. Soil profile at Mayout of Palu

Table 2: Estimation of the average shear wave velocity for array sites

No	Array Sites	Topography	Geology	Period[s]	Vs[m/s]
1	APP	Hilly	Molasse	0.6	369.7
2	GWL	Hilly	Alluvial deposits	0.56	423.7
3	KDM	Flat	Alluvial deposits	1.07	318.1
4	KRP	Flat	Alluvial deposits	1.32	318.0
5	LSS	Flat	Alluvial deposits	1.14	279.0
6	MOP	Flat	Alluvial deposits	0.59	348.0
7	MSQ	Flat	Alluvial deposits	1.23	285.7
8	SGI	Flat	Alluvial deposits	1.3	317.8

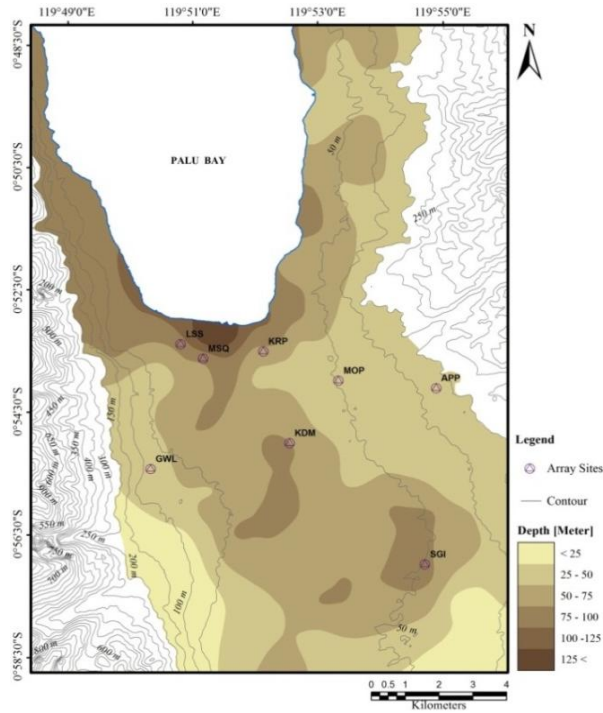


Fig.9. Depth of the engineering bed rock or sediment thickness

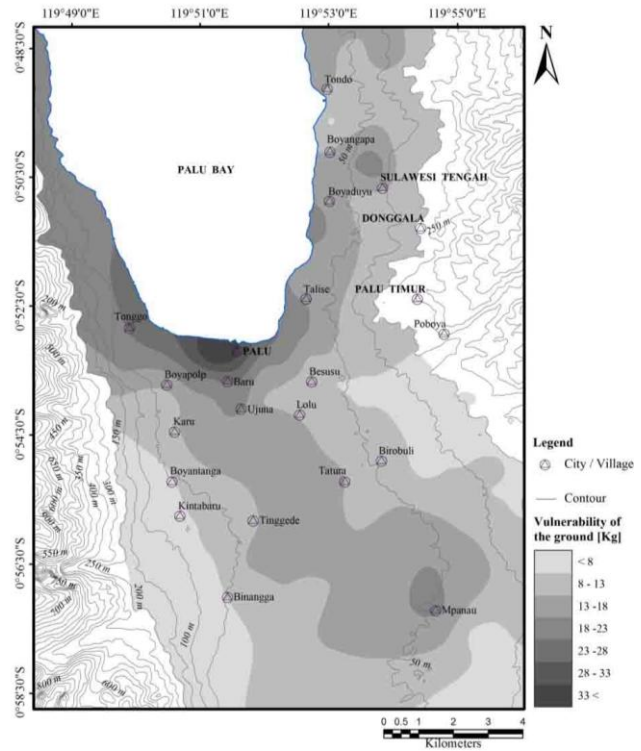


Fig. 9. The map of seismic vulnerability index of Palu City

VI. SEISMIC VULNERABILITY INDEX

Microtremor measurement has been conducted for ground structure in Palu City. For ground, the vulnerability index K_g value is calculated and verified to estimate the validity by comparing it with the past earthquake damages of 2005. In this research, microtremor measurement was conducted for ground structure to evaluate the effect of earthquake motions in the change of natural frequencies. As a result, the validity of vulnerability index obtained from the microtremor was checked by comparing it with the change of natural frequency as a quantitatively determined damage. Seismic vulnerability index is obtained by squaring the HVSr spectrum with a peak value of resonant frequency and is defined [9] as:

$$K_g = \frac{A^2}{f_0} \tag{14}$$

with K_g the seismic vulnerability A index is HVSr spectral peaks and f_0 the resonance frequency. Seismic vulnerability index is also related to geomorphological conditions showed that the high seismic vulnerability indicated that in coastal areas were composed by alluvial material. Seismic vulnerability index in Palu City found that the high seismic vulnerability indicated scattered in the alluvial and coastal deposits area. Furthermore, in the hill area, seismic vulnerability index shows a very low value. The survey results showed that in hilly areas had low seismic vulnerability index, whereas in coastal alluvium was composed of material having a high seismic vulnerability indication (Figure 9).

VII. GROUND SHEAR STRAIN

The aim of this research is to establish a simplified accurate method to evaluate the ground shear strain and vulnerability of the ground structures using microtremor. The vulnerability index is expected to be generalized as compared with actual earthquake damage. When shear deformation at ground surface at the time of earthquake is set to δ_g , the strain of surface ground γ_g is expressed as follows in approximation:

$$\gamma_g = \delta_g / h \tag{15}$$

$$\begin{aligned} &= e \times a / (2\pi F_g)^2 \times 4F_g / V_s \\ &= e \times A_g \times a / (\pi^2 F_g V_b)^2 \times V_b / V_s \\ &= \frac{A_g^2}{F_g} \times \frac{e \times a}{\pi^2 \times V_b} \\ &= K_g \times C \times a \end{aligned} \tag{16}$$

Where, $K_g = A_g^2 / F_g$ (17)

- $C = e / (\pi^2 \cdot V_b)$
- γ_g : Shear strain (in powers of 10^{-6})
- A_g : Amplification factor of the surface ground ($= V_b / V_s$)
- F_g : Natural frequency of the surface ground (Hz) $= V_s / 4h$
- a : Maximum acceleration of the basement (Gal)
- e : Efficiency of the maximum acceleration
- V_b : S-wave velocity of the basement (m/sec)
- V_s : S wave velocity of surface ground (m/sec)
- h : thickness of surface ground

Here, if it is assumed that it is $V_b \leq 1300$ m/s and $e = 0.6$, it is come to $C \approx 1.0$. Effective strain can be presumed as a value which multiplied by K_g value and the maximum acceleration in case of an earthquake. K_g value is an index

peculiar to the measured ground, and it is possible to express the vulnerability of the ground. As shown in equation (17), K_g value can be easily derived from natural frequency F_g and amplification factor A_g which were presumed in each measurement point. Figure 10 show the ground shear strain map of Palu City.

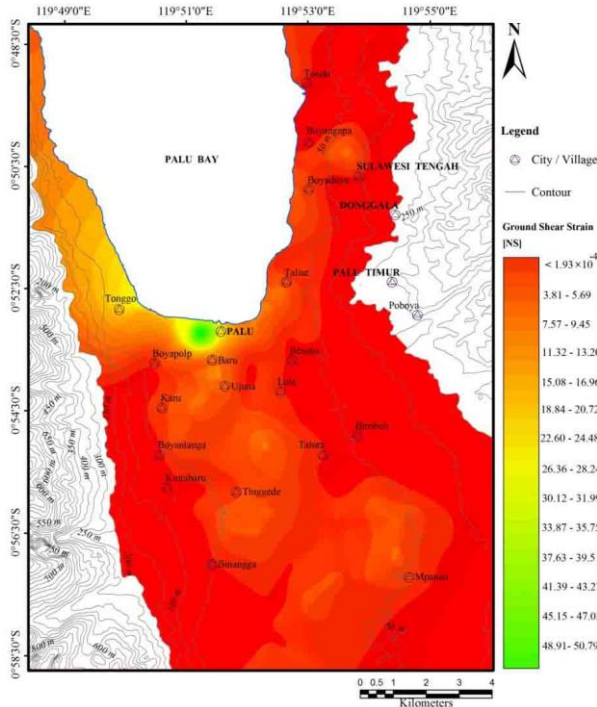


Fig. 10. Map of Ground Shear Strain (NS) in Palu City.

VIII. CONCLUSION

Our observations and analyses provide useful and practical data for earthquake disaster mitigation in Palu. The procedure employed and conclusions obtained in this study are as follows.

Microtremor observations were carried out for constructing a subsurface ground model in Palu.

Array observations were conducted at 8, which covered almost the whole city area.

The Kriging method can be used for the interpolation of subsurface information such as shear wave velocity and sediment thickness.

Microtremor survey results showed that in hilly areas had low seismic vulnerability index and ground shear strain, whereas in coastal alluvium was composed of material having a high seismic vulnerability and ground shears train indication. Palu City had deposited by fluvial depositional environment.

ACKNOWLEDGMENT

This study was supported by the Grant-in-Aid of JICA/SEED-Net. We gratefully acknowledge Dr. Noguchi, Dr. Ono in Tottori University, and Dr. RusnardiRahmat Putra in Kyoto University for their cooperation with the microtremor observations. We sincerely thank Tadulako Universities for their help in undertaking the observations in Palu, Indonesia.

REFERENCES

- [1] B. Priadi. Geochimie du magmatisme de l'Ouest du Nord de Sulawesi, Indonesia: Tracage des sources et implications geodynamique. *Doctoral thesis, Universite Paul Sabatier, Toulouse, France, 1993.*
- [2] W. Hamilton. Tectonics of the Indonesian Region, U.S. Geol. Surv. Prof. Paper 1078, 1979, 345 pp.
- [3] R. Sukanto, Reconnaissance geological map of Palu area, Sulawesi. Geological map, scale 1:250.000. Geological Survey of Indonesia, Bandaung, Indonesia, 1973.
- [4] S. Pramumijoyo, S. Indarto, C. Widiwijayanti, and J. Sopaheluwakan. Seismic Parameters of the Palu-Koro Fault in Palu Depression Area, Central Sulawesi, Indonesia, *J. SE Asian Earth Sci*, 1997.
- [5] R.A.B. Soekanto. Regional Geological Map of Palu Sheet, Indonesia, Scale 1:250,000, Geological Research Center, Bandung, 1995.
- [6] P. S. Thein, S. Pramumijoyo, K. S. Brotopuspito, W. Wilopo, J. Kiyono and A. Setianto. Investigation of Subsurface Soil Structure by Microtremor Observation at Palu, Indonesia, *The 6th ASEAN Civil Engineering Conference (ACEC) & ASEAN Environmental Engineering Conference (AEEC), Civil and Environmental Engineering for ASEAN Community*, Bangkok, Thailand. 2013, p. C-6.
- [7] T. Noguchi, T. Horio, M. Kubo, Y. Ono, J. Kiyono, T. Ikeda and P. R. Rusnardi. Estimation of Subsurface Structure in Padang, Indonesia by Using Microtremor Observation, *Report on Earthquake Disaster Prevention Field, Tono Research Institute of Earthquake Science*, Seq. No.26, 2009, pp. 1-16, (in Japanese).
- [8] J. Kiyono and M. Suzuki. Conditional Simulation of Stochastic Waves by Using Kalman Filter and Kriging Techniques, *Proc. of the 11th World Conference on Earthquake Engineering, Acapulco, Mexico*, 1996, Paper No.1620.
- [9] Y. Nakamura. Clear Identification of Fundamental Idea of Nakamura's Technique and Its Application. *World Conference of Earthquake Engineering*, 2000.

AUTHOR'S PROFILE



Mr. PyiSoe Thein

Assistant Lecturer of Geology Department, Yangon University, Myanmar. Born in Mandalay on March 1977. 2001: Bachelor degree of Geology from Geology Department, Yadanabon University, Mandalay, Myanmar. 2005: Master degree of Geology from Geology Department, Kyaukse University, Myanmar. 2008: Master degree of Computer Science from Computer Studies Department, Yangon University, Myanmar. E-mail: pyisoethein@yahoo.com



Dr. Subagyo Pramumijoyo

Professor of Geological Engineering Department, Faculty of Engineering, University of GadjahMada, Yogyakarta, Indonesia. Born in Indonesia on April 1952. 1980: Bachelor in Geological Engineering UGM, Yogyakarta. 1986: Master on Tectonophysics, Universite de Paris-Sud, France. 1991: Doctor on Geodynamics, Universite de Paris-Sud, France. 1998: Diplome in Human Resource Development, Ateneo de Manila University, Filipina E-mail: bagyo@ugm.ac.id



Dr. Kirbani Sri Brotopuspito

Professor of Physics Department, University of GadjahMada, Yogyakarta, Indonesia. E-mail: kirbani@yahoo.com



Dr. Junji Kiyono

Professor of Graduate School of Global Environmental
Studies, Kyoto University, Japan
E-mail: kiyono.junji.5x@kyoto-u.ac.jp

Dr. Wahyu Wilopo

Assistant Professor of Geological Engineering Department, Faculty of
Engineering, University of GadjahMada, Yogyakarta, Indonesia.
E-mail: wwilopo@gadjahmada.edu

Dr. Agung Setianto

Assistant Professor of Geological Engineering Department, Faculty of
Engineering, University of GadjahMada, Yogyakarta, Indonesia.
E-mail: Agung.setianto@gmail.com